Accepted Manuscript

Interlaminar toughening of woven fabric carbon/epoxy composite laminates using hybrid aramid/phenoxy interleaves

Doris W.Y. Wong, Han Zhang, Emiliano Bilotti, Ton Peijs

PII: S1359-835X(17)30227-0
DOI: http://dx.doi.org/10.1016/j.compositesa.2017.06.001
Reference: JCOMA 4688

To appear in: *Composites: Part A*

Received Date: 16 February 2017
Revised Date: 20 May 2017
Accepted Date: 3 June 2017

Please cite this article as: Wong, D.W.Y., Zhang, H., Bilotti, E., Peijs, T., Interlaminar toughening of woven fabric carbon/epoxy composite laminates using hybrid aramid/phenoxy interleaves, *Composites: Part A* (2017), doi: http://dx.doi.org/10.1016/j.compositesa.2017.06.001

Interlaminar toughening of woven fabric carbon/epoxy composite laminates using hybrid aramid/phenoxy interleaves

Doris W.Y. Wong[a], Han Zhang[a,b,*], Emiliano Bilotti[a,b], Ton Peijs[a,b,*]

[a] School of Engineering and Materials Science, and Materials Research Institute, Queen Mary University of London, Mile End Road, E1 4NS London, UK

[b] Nanoforce Technology Ltd., Joseph Priestley Building, Queen Mary University of London, Mile End Road, E1 4NS London, UK

Abstract

The influence of a hybrid interleaf system based on aramid and phenoxy fibres on the interlaminar toughness and damage tolerance of epoxy based carbon fibre reinforced plastic (CFRP) laminates was studied. An interleaf consisting of a non-woven aramid mat was either used on its own or in combination with epoxy-dissolvable thermoplastic chopped phenoxy fibres. These thermoplastic phenoxy fibres are miscible with the epoxy resin and phase separate upon curing to improve ductility and toughness. Tensile properties, Mode-I fracture toughness, interlaminar shear strength (ILSS), as well as compression after impact (CAI) properties of the toughened CFRP laminates have all been characterized and analysed. Fractography was used to identify the toughening mechanisms in the CFRP laminates with different interleaf compositions. At the optimal interleaf composition, obvious synergic effects were found in terms of the overall mechanical performance of these hybrid composite laminates, including a near 150% increment in interlaminar fracture toughness in comparison to a reference CFRP laminate.

Key words: A. Carbon fibres; A. Epoxy; A. Hybrid; B. Fracture toughness; B. Interface/interphase

* Corresponding author. Tel.: +44 020 7882 8865 (T.Peijs); +44 020 7882 2726 (H.Zhang)
E-mail address: t.peijs@qmul.ac.uk; han.zhang@qmul.ac.uk

1. Introduction

After six decades of developments since the commercialization of carbon fibre, carbon fibre reinforced plastics (CFRPs) have been widely used to replace metals in industries where high strength and stiffness are required in relation to low weight, such as aviation, automotive, automation, sports equipment, and wind energy.

Although the in-plane properties of CFRPs are generally outstanding, their relatively poor out-of-plane properties (e.g. interlaminar toughness) have often limited their wider use in structural applications due to their laminated nature. With the aim of improving their out-of-plane properties, over the years several efforts have been made to improve the toughness of epoxy matrices ranging from utilising liquid rubber [1-3] or thermoplastics [4-10], to the more recent use of nanofillers like carbon nanotubes and other nano-particles [11-17].

Although the use of liquid rubber can be regarded as one of the earliest established and most widespread toughening routes, the associated penalty of sacrificing the glass transition temperature (T_g) and Young's modulus of highly crosslinked epoxies has limited their applications in many advanced composite systems. Consequently, engineering thermoplastics of relatively high T_g have gained rapid acceptance since the late 1980s due to a better preservation of some of the advantageous properties of epoxies such as high T_g, yield stress, thermal and environmental stabilities. However, one of the major challenges encountered during the use of thermoplastic toughened resins was the increased resin viscosity and associated problems during liquid moulding processes such as resin transfer moulding (RTM) and vacuum assisted resin infusion (VARI).

The concept of localized toughening, i.e. tailoring interlaminar regions to improve mechanical properties (notably interlaminar toughness) of composite laminates without affecting resin viscosity and/or manufacturing routes, has proven itself as a successful

alternative toughening approach for many composite systems. Such toughening concepts include interlaminar hybridization with either ductile fibres like aramid [18], high-performance polyethylene [19] or ductile polymer films or interleaves [20]. The latter toughening concept was first introduced by American Cyanamid and involves the incorporation of discrete layers of a tough resin at lamina interfaces thereby giving the composite laminate the ability to undergo higher shear deformations without forming delaminations. Two main categories of thermoplastic interleaves have been employed over the years, being either epoxy-dissolvable thermoplastic films or fibres which dissolve and phase separate upon curing [21-23], or a tough interleaf that remains intact after curing [24-27].

Several research studies have been devoted to epoxy-dissolvable thermoplastic interleaves and good levels of interlaminar toughening were obtained for a number of composite systems. Yun *et al.* [23] inserted a polysulfone film as interleaf in carbon/epoxy laminates, and reported a 2.7 times higher fracture toughness than the reference laminate. Duarte *et al.* [28] utilized polyetherimide interleaves to improve the impact resistance as well as damage initiation energy of carbon/epoxy laminates. Wong *et al.* [21] reported a remarkable tenfold increase in fracture toughness with the addition of 10 wt.% phenoxy fibres into carbon fibre/epoxy laminated composites while tensile modulus, strength, and thermal stability were preserved. Zhang *et al.* [22] compared the toughening effects of phenoxy interleaves in various forms, ranging from continuous films to electrospun nanofibre mats, and explained their differences in interlaminar fracture toughness in relation to variations in dissolution times of the phenoxy interleaves as a result of different surface-to-volume ratios.

Interleaf toughening concepts in which the interlaminar region is reinforced by ductile fibres have also received a certain level of success. Sohn and Hu [24] reported a toughness improvement by adding short Kevlar® fibres (5-7 mm) to the interlaminar regions of

laminates. It was suggested that the short Kevlar® fibres acted as a fibre bridging medium between the continuous carbon fibre layers. Van Eijk and Peijs [29] reported an increase in toughness and impact behaviour of woven glass fibre reinforced plastics (GFRP) after interleaving with aramid fabrics. Yasaee *et al.* [27] employed chopped aramid fibres as interleaves to suppress damage propagation and obtained a doubling in Mode-II toughness due to the introduction of torturous crack paths and an increase in thickness of the interleaved regions. In general, it was believed that strong adhesion between interleaf and matrix and good lateral support from the intact interleaf were key to the improved mechanical performance.

Although composite interleaving with both epoxy-dissolvable thermoplastics as well as ductile polymer fibres has been successful, few attempts have been made on trying to exploit synergic effects by combining these two distinct toughening mechanisms. The possibility of combining toughening mechanisms based on shear yielding and increased plasticity for thermoplastic toughened epoxy, together with fibre bridging and crack arrest phenomena introduced through the use of ductile polymer fibres is of great interest but remained unexplored until recently.

In this work, an epoxy-dissolvable thermoplastic phenoxy, in combination with ductile aramid fibres are employed as hybrid interleaves for carbon fibre reinforced plastic (CFRP). The work builds upon excellent interlaminar toughening effects reported for interleaved systems based on chopped phenoxy fibres [21], and aims to further improve on this work through the hybridization of these phenoxy interleaves with strong and tough aramid fibres. Tensile properties, interlaminar fracture toughness, interlaminar shearing, as well as compression after impact properties of modified CFRP panels have been examined, in order to reveal potential synergistic effects between the two interleaving concepts and to provide guidelines for future novel composite designs.

2. Experimental

2.1 Materials

The composite system employed consists of a high strength (HS) plain weave carbon fibre (6K) fabric with an areal weight of 300 g/m2, supplied by Carr Reinforcements (UK) (product no. 38422), and a ACG MVR444 resin, being a tetraglycidyl 4,4-diaminodiphenylmethane (TGDDM) based epoxy resin (Figure 1a), premixed with an amine curing agent supplied by Advanced Composites Group (UK).

The phenoxy fibre (M_w ~37000 Da) was provided from Grilon® MS phenoxy yarn (500 dtex, EMS-Griltech, Switzerland), with an individual filament diameter of 48 µm. Phenoxy is a high molecular weight linear thermoplastic made by reacting bisphenol A with the diglycidyl ether of bisphenol A making it chemically similar to DGEBA epoxy resin, but with no terminal epoxide groups (Figure 1b) [30]. This phenoxy fibre was chopped to approximately 5 cm lengths prior to subsequent composite processing. The non-woven aramid interleaf veil (Optiveil®, Technical Fibre Products, UK) was made from chopped para-aramid fibres (6 mm length and 12 µm diameter), with an areal weight of 26 g/m^2 and was held together by a cross-linked polyester binder.

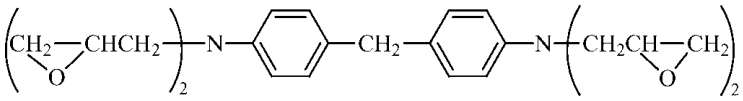

(a)

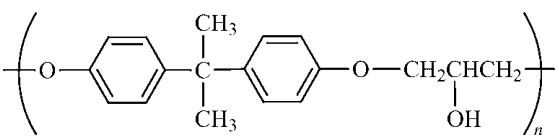

(b)

Fig. 1 Structural formula of (a) tetraglycidyl 4.4'-diaminodiphenylmethane (TGDDM) epoxy resin, and (b) phenoxy.

2.2 Sample preparation

A steel plate coated with Frekote® 700-NC release agent was used as a mould for the flat laminates. Six layers of plain weave carbon fibre fabric were cut to size (400 mm x 370 mm) and laid up in a $[0/90]_6$ configuration. A 12 μm thick polytetrafluoroethylene (PTFE) insert film was placed at the mid-plane of the lay-up for the double cantilever beam (DCB) specimens. The lay-up was sealed in a vacuum bag and the mould was heated to 80 °C before resin infusion. The premixed and degassed epoxy resin was heated to 80 °C before infusion, while the curing cycle was from 80 °C to 120 °C at 3 °C/min, holding at 120 °C for 4 hrs, followed by cooling to room temperature (RT) at 3°C /min. A post-cure was carried out in which the laminate was heated from RT to 180 °C at 3 °C/min, holding at 180 °C for 2 hrs before cooling to RT at 3 °C/min. Laminate thickness was around 2.4 mm, while the fibre volume fraction (V_f) of all laminates was around 0.5.

For phenoxy modified laminates, the phenoxy fibre was added as a chopped fibre between each layer of carbon fibre fabric. A schematic illustration is presented in Fig. 2. The phenoxy fibre content corresponded to around 5 wt.% and 10 wt.% of the total matrix content of the composite. The phenoxy fibre was weighed and randomly distributed by hand between each of the carbon fibre fabric plies. The distribution of phenoxy fibres in terms of areal weight was around 12.5 g/m^2 and 25 g/m^2 for the 5 wt.% and 10 wt.% phenoxy specimens, respectively. It is worth noting that for future applications a more consistent and homogeneous distribution of phenoxy within the laminates could be obtained by utilising non-woven phenoxy fibre mats. Upon impregnation with unmodified TGDDM epoxy resin

and subsequent curing, these phenoxy fibres are expected to dissolve and phase separate to form a secondary thermoplastic phase that toughens the epoxy matrix at the inter-ply region. The preparation of the mould, sealing of the vacuum bag, mixing of the resin and curing agent, and the resin infusion process were all as described above.

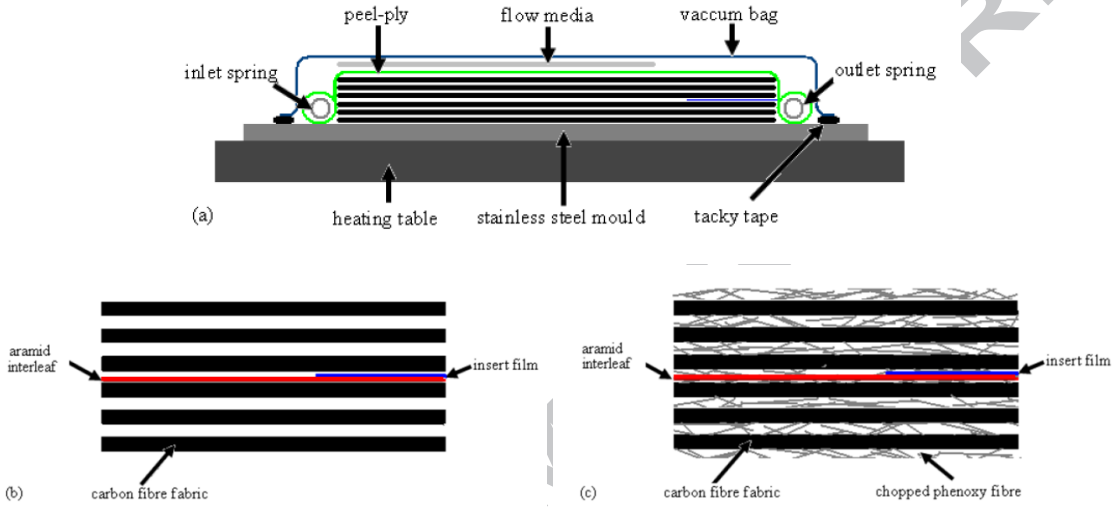

Fig. 2 Schematic illustration of (a) vacuum assisted resin infusion (VARI) process, (b) location of non-woven aramid interleaf (in red), and (c) location of chopped phenoxy fibres (in grey).

For comparison, neat epoxy resin specimens and modified epoxy blends with 5 wt.% and 10 wt.% phenoxy were also manufactured. For this purpose, epoxy resin was heated to 130 ºC before adding the phenoxy fibres and curing agent. The epoxy/phenoxy mixture was stirred until homogeneous and transparent after which the curing agent was added. This mixture was then poured into an open PTFE mould and degassed in a vacuum oven. Samples were cured using the same curing cycle as for the composites. A dog-bone shaped mould was used for the preparation of tensile specimens according to ASTM 638 Type V, while a rectangular

mould was used to for fracture toughness specimens, which were cut to size (30 mm x 6 mm x 3 mm), after curing.

2.3 Characterizations

Tensile testing

For tensile testing, the composite laminates were cut to size (200 mm x 20 mm x 2.4 mm) using a diamond cutting wheel, with glass fabric reinforced epoxy end-tabs (38 mm x 20 mm) adhesively bonded to both ends and tested in accordance to ASTM D3039 [31]. A strain gauge with a length of 6 mm was bonded to the centre of each specimen using an epoxy adhesive. The tests were performed using an Instron 5505 universal testing machine equipped with a 100 kN load cell at a rate of 2 mm/min. Neat resin dog-bone specimens were tested according to ASTM 638, using an Instron universal testing machine equipped with a 10 kN load cell and an optical extensometer at a test speed of 1 mm/min. Five specimens were tested for each type of material system.

Fracture toughness

Double cantilever beam (DCB) specimens were prepared for Mode-I interlaminar fracture toughness tests in accordance with ASTM D5528 [32]. The composite laminates were cut to size (130 mm x 20 mm x 2.4 mm) and a composite material made of glass fabric and epoxy (similar as used for end-tabs) was cut to size (130 mm x 20 mm) and bonded to both sides of the specimen surface to increase flexural stiffness, making the total thickness of the specimens around 6 mm. Piano hinges were bonded to the ends of the specimens, and the distance between the loading points and the end of the PTFE insert film (i.e. the beginning of the crack) was 50 mm. The sides of the specimens were spray painted with a white paint primer and markers were drawn on the primer for every 1 mm interval. Each sample was

loaded in Mode-I tension using a Hounsfield universal testing machine at a rate of 1 mm/min. Crack growth was observed using a digital microscope and the loads and displacements at corresponding crack lengths were recorded. The G_{IC} values in this study were calculated using the modified beam theory (MBT) and refer to propagation G_{IC} values. MBT was selected since it yielded the most conservative values for the majority of test cases evaluated in a round robin test carried out by the ASTM [32]. Fracture toughness tests on neat resin specimens were carried out in accordance with ASTM D5045, using a single notched three-point bending specimen (30 mm x 6 mm x 3 mm). A notch, 2 mm deep, was machined in the middle of one side of the specimen before a fresh, sharp razor blade was slid repeatedly across the notch to create a total notch depth of 3 mm. Three-point bending tests were carried out using an Instron universal testing machine at a test speed of 1 mm/min and a span-to-thickness ratio of 4. Five specimens of each type were tested.

Interlaminar shear strength

In this study, the interlaminar shear strength (ILSS) of the hybrid laminates was measured using the short beam shear (SBS) test method in accordance with ASTM D2344 [33], using an Instron universal testing machine at a test speed of 1 mm/min. The width-to-thickness ratio of the specimen was 2 while the span-to-thickness ratio was 4. The average dimensions of the SBS specimens were 25 mm x 4.4 mm x 2.4 mm. The diameters of the loading and supporting rollers were 6 mm and 3 mm, respectively. A detailed illustration can be found in [34].

Compression after impact

In this study compression after impact (CAI) specimens were cut from composite panels to size (90 mm x 55 mm x 2.4 mm) and impacted at 2, 4 and 6 Joules, using a CEAST impact tester. Each specimen was clamped in a 40 mm diameter support and the dart diameter was 20 mm. The non-impacted and impacted specimens were then placed in a miniaturised

Boeing CAI rig [35] and loaded in compression at a rate of 0.5 mm/min. Five specimens were tested for each impact energy. The maximum compressive strength was recorded and presented as the compression after impact (CAI) strength.

Fractography

The Mode-I fracture surfaces of specimens were examined in a scanning electron microscope (SEM), Inspect^{TM} F from FEI Company (Netherlands). Specimens were coated with gold prior to imaging, and an electron beam of 20 kV was used.

3. Results and Discussions

3.1 Fractography

Fig. 3a shows a typical brittle fracture surface of a non-modified TGDDM epoxy matrix. With the addition of 5 wt.% and 10 wt.% phenoxy this single-phase epoxy system is changed into an epoxy blend with a dispersed morphology consisting of phenoxy droplets in a TGDDM epoxy matrix (Figs. 3b, c). The main toughening mechanisms from phenoxy modification are believed to be the particle-induced shear yielding, which contributes to energy dissipation during crack propagation. These morphological observations are in agreement with previous epoxy/phenoxy studies by Siddhamalli and Kyu [35], who reported a dispersed droplet morphology for phenoxy concentrations of 10 wt.%, while a co-continuous morphology was observed for 20 wt.% phenoxy. A phase inverted morphology was obtained for phenoxy concentrations of 30 wt.% and above.

Figs. 3d, e and f show Mode-I fracture surfaces of carbon/epoxy laminates without and with phenoxy. Already with the presence of 5 wt.% phenoxy, a clear morphological change from a typical brittle Mode-I fracture surface for neat epoxy (Fig. 3d) to a more deformed and rough surface for the blend was observed (Fig. 3e). Brittle fracture from Mode-I failure in neat

epoxy based laminates was characterized by a smooth corrugated fracture surface, which is partly the result of fibre debonding.

Fig. 3g shows the morphology of Mode-I fracture surfaces of aramid veil interleaved specimens without phenoxy. Clearly, most interlaminar cracking occurs at the carbon/epoxy interface as indicated by the exposed carbon fibre fabric, indicating that the involvement of the aramid fibre interleaf in the overall failure process is rather negligible. Fracture surfaces of aramid interleaved laminates with 5 wt.% phenoxy at inter-ply regions (Fig. 3h), showed a significant changed in failure mode compared to the neat resin based composite system, with the aramid fibres now contributing more to the interlaminar failure process. Apparently a better load transfer and connectivity between the carbon fibre plies and the non-woven aramid veil was achieved with the introduction of the phenoxy, leading to increased aramid fibre pull-out, fibre bridging and fibrillation. Similar levels of matrix and aramid fibre deformation were observed in laminates based on 10 wt.% phenoxy (Fig. 3i). Morphological studies did not reveal a clear co-continuous or phase-inverted blend morphology in the composites at the current phenoxy loadings, although local phenoxy concentrations in interlaminar regions are expected to be well above the overall concentration of 5 and 10 wt.%.

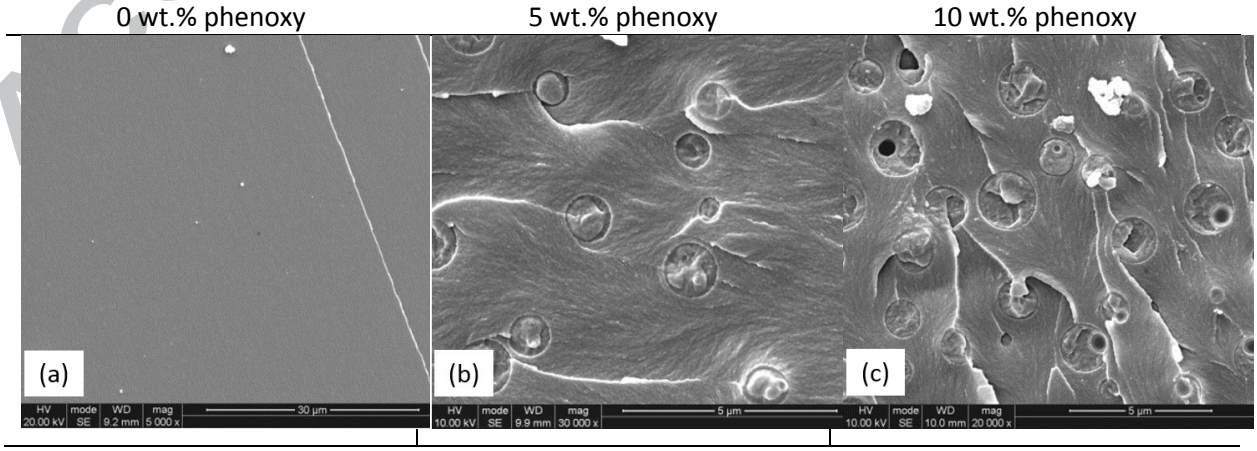

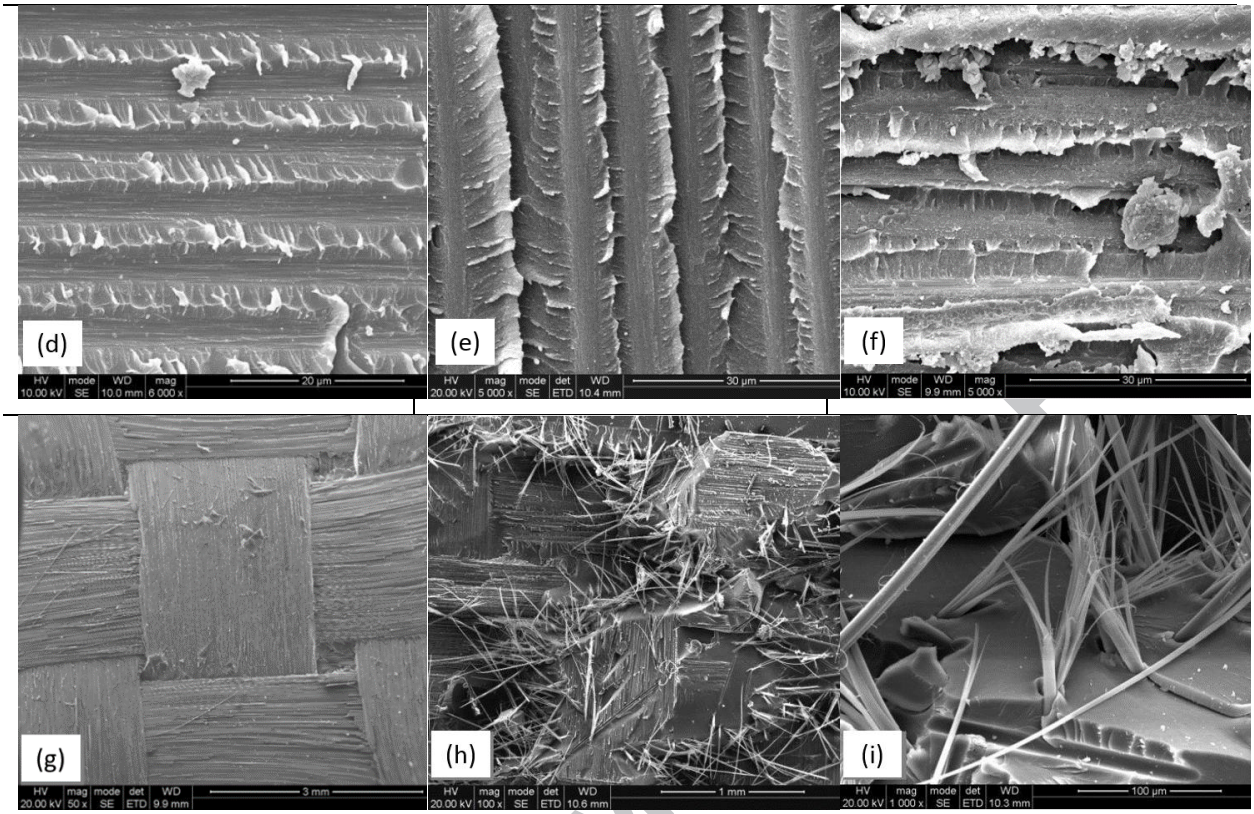

Fig. 3 SEM image of Mode-I fracture surfaces of phenoxy/epoxy blends at different phenoxy concentrations of: (a) neat epoxy resin; (b) 5 wt.% phenoxy and (c) 10 wt.% phenoxy, showing a slightly rougher fracture surface with a droplet morphology after phase separation. Mode-I interlaminar fracture surfaces of phenoxy modified CFRP laminates at different phenoxy concentrations of: (d) neat epoxy resin, showing brittle failure features together with fibre debonding; (e) 5 wt.% phenoxy and (f) 10 wt.% phenoxy, showing more ductile failure. And finally, Mode-I interlaminar fracture surfaces of aramid veil interleaved CFRP laminates of: (g) neat epoxy resin, showing negligible involvement of the aramid veil interleaf; (h) 5 wt.% phenoxy and (i) 10 wt.% phenoxy, showing a significantly increased contribution of the aramid veil via fibre pull-out, fibrilation and fibre bridging, confirming the improved contribution of the aramid interleaf to the interlaminar fracture process in the presence of phenoxy.

3.2 Tensile properties

It is well known that the in-plane properties of CFRPs are dominated by the continuous carbon fibres. Hence it is expected that the addition of a non-woven aramid interleaf at the mid-ply as well as matrix modification by phenoxy will not significantly affect the tensile properties of the CFRP laminates. However, a reduction in effective carbon fibre volume fraction with interleaving may lead to less load carrying carbon fibres per unit area, which could lead to a slight reduction in strength and stiffness.

Fig. 4 shows the tensile properties of both reference and interleaved CFRP laminates. As expected, the tensile modulus was only slightly reduced with the introduction of the aramid interleaf, while the addition of phenoxy did not significantly affect the Young's modulus of the laminates as well as that of the neat epoxy system (see Table 1). A similar trend was found for the tensile strength of the aramid interleaved CFRP panels. Interestingly, here the addition of 10 wt.% phenoxy to the epoxy resin resulted in a slight increase in tensile strength compared to the reference laminate, indicating a certain level of synergy between the two interleaf systems.

The macroscopic failure modes of all interleaved specimens were similar (Fig. 5). All specimens fractured across their width with limited evidence of delamination, regardless of the interleaf system present. Some evidence of fibre debonding was noted for both reference and 5 wt.% phenoxy modified specimens. It can be expected that apart from the carbon fibre content, the interfacial adhesion between the carbon fibre/epoxy and aramid fibre/epoxy plays an important role in the tensile properties.

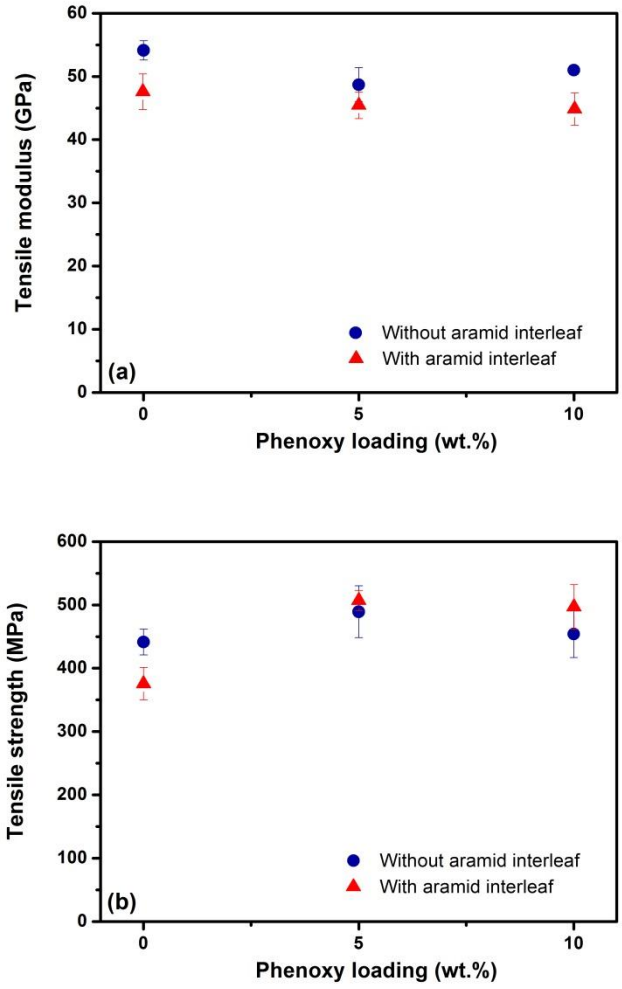

Fig. 4 (a) Young's modulus and (b) tensile strength of CFRP laminates with and without a non-woven aramid interleaf and different phenoxy concentrations.

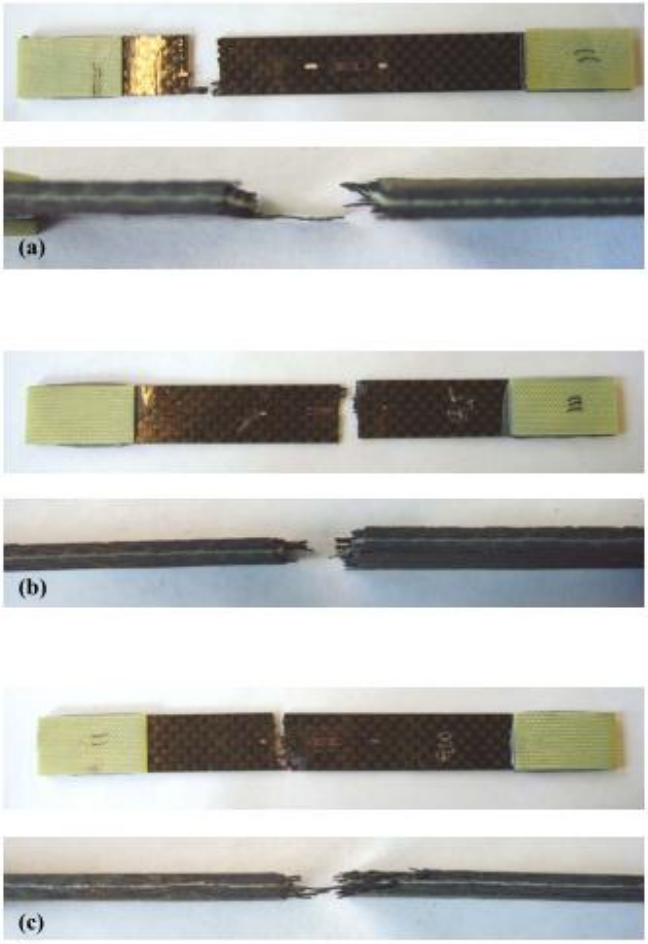

Fig. 5 CFRP test specimens with non-woven aramid interleaf and (a) 0 wt.%; (b) 5 wt.%; and (c) 10 wt.% phenoxy, showing similar macroscopic failure modes.

3.3 Interlaminar fracture toughness

With the aim of having a baseline of the current phenoxy modified epoxy systems, the mechanical properties of the phenoxy/epoxy blends are summarised in Table 1. At current phenoxy concentrations the mechanical properties of the epoxy blends are not greatly affected by the presence of phenoxy. Although the fracture toughness of the blends was increased between 10 and 40%, all systems exhibited relatively similar levels of toughness due to epoxy being the continuous phase. Similar levels of toughness (K_{1c}) of around 0.7 MPa/m^2 for neat epoxy and 0.9 MPa/m^2 for blends consisting of 10 wt.% phenoxy and

exhibiting a droplet morphology were reported by Siddhamalli and Kyu [35]. However, their study also revealed significantly increased fracture toughness levels of around 3.2 MPa/m^2 for slightly higher phenoxy concentrations of 20 wt.% as a result of a co-continuous blend morphology. A further increase in phenoxy content to 30 wt.% resulted in a phase-inverted morphology but slightly lower fracture toughness levels of around 2.3 MPa/m^2 [35].

Table 1. Summary of mechanical properties of phenoxy/epoxy blends.

	Modulus (GPa)	Strength (MPa)	K_{IC} (MPa/m^2)	G_{IC} (kJ/m^2)
Epoxy	3.2 (±0.4)	80.3 (±20)	0.66 (±0.13)	0.09 (±0.02)
5 wt.% phenoxy	3.0 (±0.3)	68.2 (±8)	0.95 (±0.01)	0.13 (±0.01)
10 wt.% phenoxy	3.4 (±0.2)	68.4 (±15)	0.80 (±0.12)	0.10 (±0.03)

The interlaminar fracture toughness of laminated composites is normally expressed in terms of critical energy release rate, G_c, and is the energy consumed by the material as the delamination front advances through a unit area. The Mode-I interlaminar fracture toughness of CFRP laminates without aramid or phenoxy was first tested as a reference. Fig. 6a shows the load-displacement (L-D) curves as well as the toughness and crack length increment (R-curve) for the reference laminate and panels with two phenoxy concentrations. Typical L-D curves can be seen, with step-like load increments and sudden load drops near the end of the test. In comparison to the reference panel, the addition of 5 wt.% phenoxy results in no obvious change in the L-D curve. However, with the addition of 10 wt.% phenoxy, an obvious increasing trend in the L-D curve can be seen, indicating that a larger amount of energy is required to propagate the crack. This trend was confirmed by the R-curves in Fig. 6a, suggesting that the addition of 10 wt.% phenoxy significantly enhanced the interlaminar toughness of the CFRP laminates. The similarity in interlaminar toughness of composite

laminates based on neat epoxy and 5 wt.% phenoxy blend is in agreement with the pure matrix systems, which revealed no significant differences in toughness between these two blends. Mode-I fracture toughness values of composite laminates were somewhat higher than those of the polymer matrix presumably due to effects such as fibre debonding and fibre bridging, all of which can lead to an increase in fracture surface area. Interestingly, composite laminates based on blends incorporating 10 wt.% phenoxy showed a step change in interlaminar toughness, not observed in the pure matrix system. In fact, interlaminar toughness values for these laminates are more in line with values reported by Siddhamalli and Kyu for blends containing 20 and 30 wt.% phenoxy [35]. This suggests a change in blend morphology from phenoxy droplets to a co-continuous or phase inverted morphology in these composites. Since the phenoxy in the composite laminates is highly localized within the interlaminar regions it can be easily envisaged that local phenoxy concentrations are indeed significantly higher than the overall concentration of 10 wt.%. This could lead to a change in blend morphology within these regions and a significant change in interlaminar toughness.

Fig. 6b shows the L-D curves and R-curves of the aramid interleaved panels. Apparently, here for both phenoxy loadings, the load required for crack initiation and propagation was increased and R-curves remained high after the introduction of the non-woven aramid veil for both phenoxy loadings. It is worth noting that the initiation values for the aramid interleaved panels were slightly lower than for panels without aramid interleaf, which was subsequently recovered and further improved after the introduction of phenoxy, suggesting a synergic effect between epoxy, phenoxy and aramid fibres. The likely cause of this initial drop is believed to be due to relatively poor interfacial bonding between the aramid veil and epoxy matrix as suggested by the fracture surface shown in Fig 3g, and which was subsequently improved with the introduction of phenoxy (see Figs. 3h, i), leading to an increase in energy absorption processes such as aramid fibre pull-out, fibrillation and bridging.

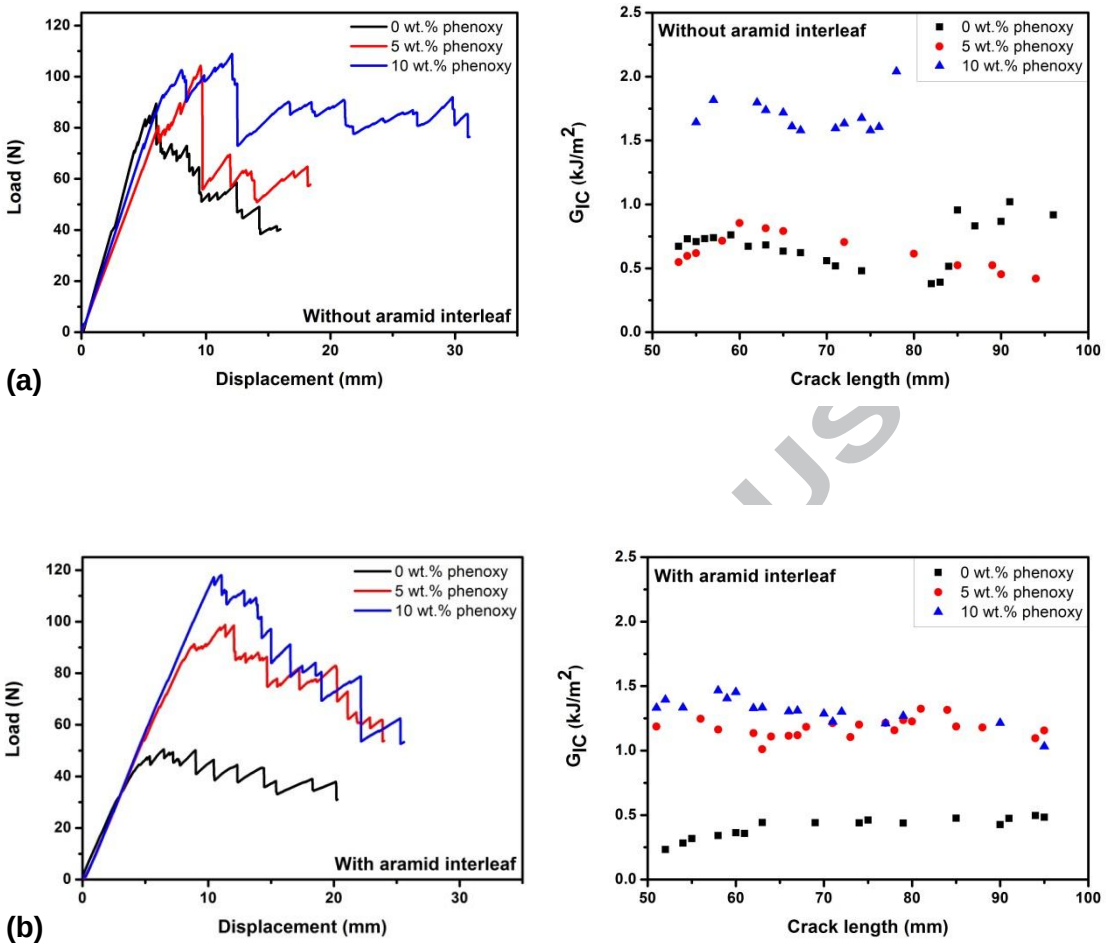

Fig. 6 Double cantilever beam (DCB) load-displacement curves (left) and R-curves (right) of: (a) carbon fibre/epoxy laminates without aramid interleaf and different phenoxy concentrations; and (b) carbon fibre/epoxy laminates with aramid interleaf and different phenoxy concentrations.

To have a more clear comparison, the calculated interlaminar fracture toughness values (G_{IC}) are plotted in Fig. 7 for all laminates. As mentioned earlier, the G_{IC} value is an indication of how much energy is required to propagate the interlaminar crack. Without aramid interleaf, no obvious difference was observed for the reference CFRP panel and the panel with 5 wt.%

phenoxy, while a significantly higher G_{IC} value was measured for the panel with 10 wt.% phenoxy.

As mentioned earlier, the interlaminar fracture toughness was slightly reduced when an aramid interleaf was introduced in the neat epoxy based laminate. This reduction could be attributed to the relatively poor integration of the aramid veil (see Fig. 3g), possibly partly as a result of the presence of the crosslinked polyester binder on the aramid fibres. Because of this, it might be beneficial in future to use an epoxy soluble binder (such as phenoxy) for aramid veils in this type of application.

Both 5 wt.% and 10 wt.% phenoxy modified laminates showed an apparent increase in G_{IC} values, especially for 5 wt.% phenoxy based specimens where a doubling in interlaminar fracture toughness was achieved for aramid interleaved laminates. As mentioned before, this increment is believed to be attributed to an improved integration of aramid fibres with phenoxy modification. The highest G_{IC} value was obtained after the introduction of both the aramid interleaf and phenoxy, suggesting a possible synergic toughening effect between these two systems.

This synergic effect was consistent with morphological observations shown in Fig. 3. For laminates without phenoxy, debonding occurred at the carbon/epoxy interface with limited interaction between the woven carbon fabric and the non-woven aramid veil. On the other hand, laminates with both 5 wt.% and 10 wt.% phenoxy revealed a much better interaction between carbon and aramid, and failure modes that involved both fibres. For these hybrid systems, fibre debonding and fibre pull-out occurred for both fibres, together with some fibre breakage of carbon fibres, and fibre fibrillation and splitting of aramid fibres. These observations suggest a favourable interaction between carbon and aramid fibres in the case of

phenoxy modified epoxy systems, which allowed for the contribution of both fibres to the overall laminate toughness.

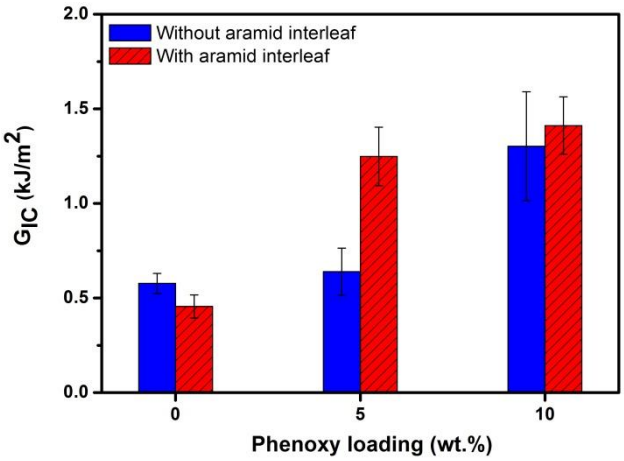

Fig. 7 Comparison of the Mode-I interlaminar fracture toughness of CFRP laminates with and without aramid interleaf and different phenoxy concentrations, showing the importance of the presence of a small amount of phenoxy phase to fully utilize the toughening potential of the non-woven aramid interleaf.

3.4 Interlaminar shear strength

In composite materials, a low resistance to shear deformation, especially for matrix dominated properties is a severe weakness. Relatively low shear stiffness and strength often compromise a composite materials' performance. Interlaminar shear strength (ILSS) is strongly dependent on the stress transfer capability of the fibre/matrix interface and therefore sometimes used as a qualitative indicator for the level of interfacial bonding in laminated composites. Composites with low ILSS values are prone to delamination and often have a poor resistance to environmental degradation, which is detrimental to many applications. However, composites with too high ILSS values may have a lower toughness, as some of the

toughening mechanisms such as fibre/matrix debonding and crack deflection cannot be triggered.

The interlaminar shear strength was determined from the short beam shear (SBS) test and is plotted in Fig. 8. Without aramid interleaf, no obvious changes in ILSS were observed for phenoxy modified laminates. After the introduction of the aramid interleaf, a reduction in ILSS value was observed for neat epoxy systems without phenoxy, which is consistent with the previous Mode-I fracture toughness trends. For 5 wt.% phenoxy modified laminates and aramid interleaves, the ILSS value was obviously increased, while a further increase in phenoxy content (10 wt.%) did not lead to a further increase in ILSS. However, overall the introduction of phenoxy led to a respectable improvement in ILSS for CFRP laminates with aramid interleaving.

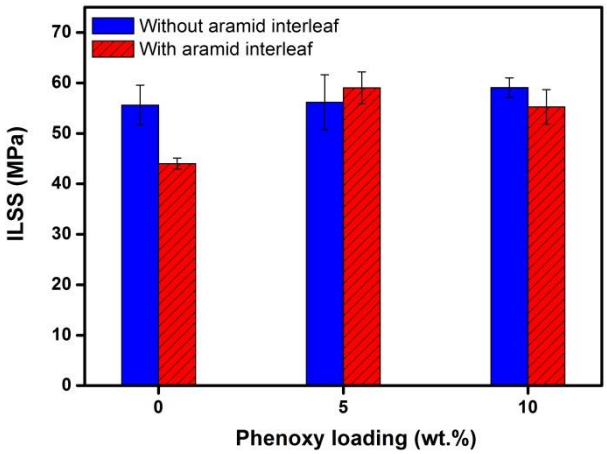

Fig. 8 Comparison of interlaminar shear strength (ILSS) of CFRP laminates with and without aramid interleaf and different phenoxy concentrations.

3.5 Compression after impact

Impact resistance and damage tolerance are very important considerations for composite laminates, as impact loadings can result in non-visible damage and reduced residual properties. It is important to understand how a composite will perform after being damaged. The compression after impact (CAI) test for composite laminates generally involves subjecting a plate to an out-of–plane low energy impact to introduce damage but not complete failure. The damaged plate will then be loaded until failure by in-plane compression. The most common form of internal damage after impact is delamination. Delamination can lead to premature failure during compression loading caused by ply buckling and Mode-I dominated crack growth.

In this work, each specimen was subjected to a non-penetrating impact of 2, 4 and 6 Joules, followed by compression after impact (CAI) tests to examine their residual compressive properties (Fig. 9). Regardless of the impact energy applied, an increased compression after impact (CAI) strength was obtained from all laminates with the introduction of both phenoxy and aramid interleaf. In the case of laminates based on neat epoxy resin the addition of an aramid interleaf resulted in a reduction in CAI strength, presumably due to the formation of sub-laminates as a result of impact induced delaminations. This trend is consistent with the previously reported Mode-I fracture toughness and short beam shear data (see Figs. 7 and 8), which showed reduced G_{IC} and ILSS values with the introduction of an aramid interleave for neat epoxy based panels. Conversely, an obvious increase in CAI strength was observed with the introduction of an aramid interleaf for panels based on phenoxy modified epoxy, in particular for systems with 5 wt.% phenoxy were a clear synergistic effect was observed for laminates incorporating an aramid interleaf and phenoxy as a toughening agent. Again this trend is consistent with the G_{IC} and ILSS data in Figs. 7 and 8. This seems to suggest a link between CAI strength and interlaminar fracture toughness and/or interlaminar shear strength.

It is well know that delamination growth under impact is controlled by a combined Mode-I crack opening action and a Mode-II shear action [36]. Hence, it is not surprising that residual compressive strength after impact, which is strongly controlled by buckling of delaminated sub-laminates, follows similar trends as Mode-I dominated DCB and Mode-II dominated SBS data.

Finally, it should be noted that the highest overall residual compressive properties were measured for aramid interleaved CFRP laminates based on phenoxy modified epoxy, again highlighting the importance of phenoxy in this hybrid toughening concept.

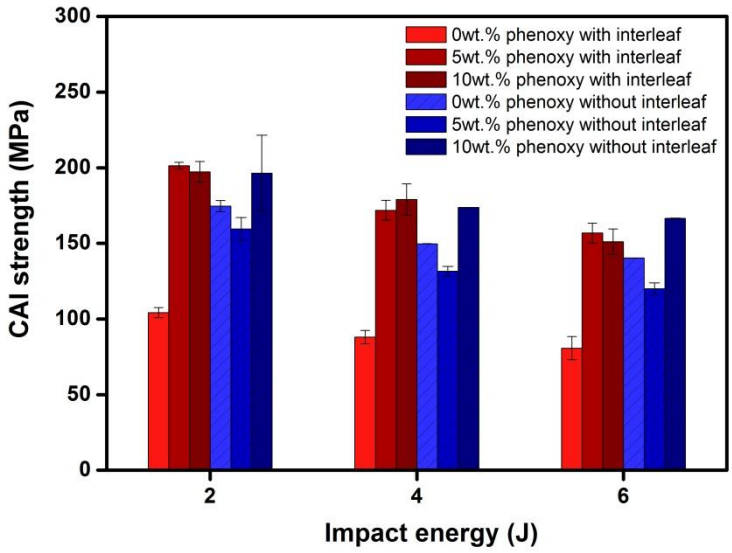

Fig. 9 Comparison of residual compressive after impact (CAI) strength for CFRP laminates with and without aramid interleaf and different phenoxy concentrations.

4. Conclusions

The combined action of two interleaf based toughening concepts for CFRP has been investigated in this experimental study. Two distinct interleaf and toughening mechanisms were employed: (i) phenoxy fibre interleaves which dissolved and phase separated upon

curing to improve the epoxy resin ductility and toughness within the interlaminar region; and (ii) a non-woven aramid interleaf to improve the toughness within the interlaminar region by fibre bridging and crack arrest. Tensile and compressive properties, as well as out-of-plane interlaminar properties were examined for CFRP laminates for these two types of toughening concepts.

A synergistic toughening effect was found when combining phenoxy and aramid interleaves, leading to a high damage tolerance as measured in compression after impact, while various toughening mechanisms were identified from fractographic studies. Interestingly, the presence of phenoxy improved the interfacial properties between the woven fabric carbon plies and the non-woven aramid interleaf, leading to enhanced load transfer and hence improved interlaminar properties and impact damage tolerance.

Based on the understanding obtained from this hybrid interleaving methodology, together with previous studies on dissolvable phenoxy systems [21, 22], the current hybrid interleaving system could be extended to various other thermoplastic toughening agents for application in both carbon- and glass fibre reinforced plastics.

References:

[1] Kinloch AJ, Shaw SJ, Tod DA, Hunston DL. Deformation and fracture-behavior of a rubber-toughened epoxy .1. microstructure and fracture studies. Polymer. 1983;24(10):1341-1354.
[2] Chikhi N, Fellahi S, Bakar M. Modification of epoxy resin using reactive liquid (ATBN) rubber. Eur Polym J. 2002;38(2):251-264.
[3] Thomas R, Yumei D, Yuelong H, Le Y, Moldenaers P, Weimin Y, et al. Miscibility, morphology, thermal, and mechanical properties of a DGEBA based epoxy resin toughened with a liquid rubber. Polymer. 2008;49(1):278-294.
[4] Bucknall CB, Gilbert AH. Toughening tetrafunctional epoxy-resins using polyetherimide. Polymer. 1989;30(2):213-217.
[5] Mackinnon AJ, Jenkins SD, McGrail PT, Pethrick RA. A dielectric, mechanical, rheological, and electron-microscopy study of cure and properties of a thermoplastic-modified epoxy-resin. Macromolecules. 1992;25(13):3492-3499.

[6] Pethrick RA, Hollins EA, McEwan I, MacKinnon AJ, Hayward D, Cannon LA, et al. Dielectric, mechanical and structural, and water absorption properties of a thermoplastic-modified epoxy resin: Poly(ether sulfone)-amine cured epoxy resin. Macromolecules. 1996;29(15):5208-5214.
[7] DiPasquale G, Motta O, Recca A, Carter JT, McGrail PT, Acierno D. New high-performance thermoplastic toughened epoxy thermosets. Polymer. 1997;38(17):4345-4348.
[8] Zhang H, Liu Y, Huang M, Bilotti E, Peijs T. Dissolvable thermoplastic interleaves for carbon nanotube localization in carbon/epoxy laminates with integrated damage sensing capabilities. Structural Health Monitoring. 2016:DOI:10.1177/1475921716683653.
[9] Venderbosch RW, Peijs T, Meijer HEH, Lemstra PJ. Fibre-reinforced composites with tailored interphases using PPE/epoxy blends as a matrix system. Compos Pt A-Appl Sci Manuf. 1996;27(9):895-905.
[10] Saalbrink A, Lorteije A, Peijs T. The influence of processing parameters on interphase morphology in polymer composites based on phase-separating thermoplast/epoxy blends. Compos Pt A-Appl Sci Manuf. 1998;29(9-10):1243-1250.
[11] Kinloch AJ, Mohammed RD, Taylor AC, Eger C, Sprenger S, Egan D. The effect of silica nano particles and rubber particles on the toughness of multiphase thermosetting epoxy polymers. J Mater Sci. 2005;40(18):5083-5086.
[12] Hsieh TH, Kinloch AJ, Masania K, Lee JS, Taylor AC, Sprenger S. The toughness of epoxy polymers and fibre composites modified with rubber microparticles and silica nanoparticles. J Mater Sci. 2010;45(5):1193-1210.
[13] Zhang H, Liu Y, Kuwata M, Bilotti E, Peijs T. Improved fracture toughness and integrated damage sensing capability by spray coated CNTs on carbon fibre prepreg. Compos Pt A-Appl Sci Manuf. 2015;70:102-110.
[14] Fong H, Chun I, Reneker DH. Beaded nanofibers formed during electrospinning. Polymer. 1999;40(16):4585-4592.
[15] Inam F, Wong DY, Kuwata M, Peijs T. Multiscale Hybrid Micro-Nanocomposites Based on Carbon Nanotubes and Carbon Fibers. J Nanomater. 2010.
[16] Zhang H, Kuwata M, Bilotti E, Peijs T. Integrated damage sensing in fibre-reinforced composites with extremely low carbon nanotube loadings. J Nanomater. 2015;2015(Article ID 785834):7.
[17] Zhang H, Bilotti E, Peijs T. Nano-Engineered Hierarchical Carbon Fibres and Their Composites: Preparation, Properties and Multifunctionalities. In: Beaumont PWR, Soutis C, Hodzic A, editors. The Structural Integrity of Carbon Fiber Composites: Fifty Years of Progress and Achievement of the Science, Development, and Applications, Cham: Springer International Publishing; 2017. p. 101-116.
[18] Marom G, Drukker E, Weinberg A, Banbaji J. Impact Behavior of Carbon Kevlar Hybrid Composites. Composites. 1986;17(2):150-153.
[19] Peijs AAJM, Venderbosch RW. Hybrid composites based on polyethylene and carbon fibres Part IV Influence of hybrid design on impact strength. Journal of Materials Science Letters. 1991;10(19):1122-1124.
[20] Evans RE, Masters JE. A New Generation of Epoxy Composites for Primary Structural Applications: Materials and Mechanics. ASTM Toughened Composite Symposium, Houston, Tex, USA: ASTM International; Jan 1987. p. 413-436.
[21] Wong DWY, Lin L, McGrail PT, Peijs T, Hogg PJ. Improved fracture toughness of carbon fibre/epoxy composite laminates using dissolvable thermoplastic fibres. Compos Pt A-Appl Sci Manuf. 2010;41(6):759-767.
[22] Zhang H, Bharti A, Li Z, Du S, Bilotti E, Peijs T. Localized toughening of carbon/epoxy laminates using dissolvable thermoplastic interleaves and electrospun fibres. Composites Part A: Applied Science and Manufacturing. 2015;79:116-126.
[23] Yun NG, Won YG, Kim SC. Toughening of carbon fiber/epoxy composite by inserting polysulfone film to form morphology spectrum. Polymer. 2004;45(20):6953-6958.
[24] Sohn M-S, Hu X-Z. Mode II delamination toughness of carbon-fibre/epoxy composites with chopped Kevlar fibre reinforcement. Compos Sci Technol. 1994;52(3):439-448.

[25] Gustin J, Joneson A, Mahinfalah M, Stone J. Low velocity impact of combination Kevlar/carbon fiber sandwich composites. Compos Struct. 2005;69(4):396-406.
[26] Yasaee M, Bond IP, Trask RS, Greenhalgh ES. Mode I interfacial toughening through discontinuous interleaves for damage suppression and control. Compos Pt A-Appl Sci Manuf. 2012;43(1):198-207.
[27] Yasaee M, Bond IP, Trask RS, Greenhalgh ES. Mode II interfacial toughening through discontinuous interleaves for damage suppression and control. Composites Part A: Applied Science and Manufacturing. 2012;43(1):121-128.
[28] Duarte A, Herszberg I, Paton R. Impact resistance and tolerance of interleaved tape laminates. Compos Struct. 1999;47(1–4):753-758.
[29] R. Van Eijk TP. Impact behaviours of glass/aramid hybrid composites. In: A. Poursartip KSE, editor. 10th international conference on composites materials (ICCM-10), vol. 5 Whistler (BC), Canada: Woodhead Publ. Ltd; 1995. p. 599.
[30] Zhang H, Bilotti E, Tu W, Lew CY, Peijs T. Static and dynamic percolation of phenoxy/carbon nanotube nanocomposites. Eur Polym J. 2015;68(0):128-138.
[31] ASTM-D-3039-00. ASTM D3039-00 Standard Test Method for Tensile Properties of Polymer Matrix Composite Materials. ASTM International. 2000.
[32] ASTM-D-5528-01. Mode I interlaminar fracture toughness of unidirectional fiber-reinforced polymer matrix composites, technical report. American Society for Testing and Materials International, 2007.
[33] ASTM-D2344. Standard Test Method for Short-Beam Strength of Polymer Matrix Composite Materials and Their Laminates. ASTM International.
[34] Zhang H, Liu Y, Bilotti E, Peijs T. In-situ monitoring of interlaminar shear damage in carbon fibre composites. Adv Compos Lett. 2015;24(4):92-97.
[35] Prichard JC, Hogg PJ. The role of impact damage in post-impact compression testing. Composites. 1990;21(6):503-511.
[36] Kim JK, Sham ML. Impact and delamination failure of woven-fabric composites. Compos Sci Technol. 2000;60(5):745-761.